Hindawi
International Journal of Aerospace Engineering
Volume 2022, Article ID 1245484, 9 pages
https://doi.org/10.1155/2022/1245484

Research Article

Lift Enhancement of Tiltrotor Wing Using a Gurney Flap

Hao Chen [1] **and Bo Chen** [2]

[1]*Jiangsu Key Laboratory of Advanced Manufacturing Technology, Huaiyin Institute of Technology, 223003 Huaian, Jiangsu, China*
[2]*Water Conservancy Bureau of Hongze District, 223100 Huaian, Jiangsu, China*

Correspondence should be addressed to Hao Chen; chenhao@hyit.edu.cn

Received 2 October 2021; Revised 29 November 2021; Accepted 30 December 2021; Published 21 January 2022

Academic Editor: Andre Cavalieri

A numerical investigation was undertaken to explore the lift-enhancing characteristics of the Gurney flap on a tiltrotor wing. The heights of Gurney flaps range from 1 to 4% wing chord lengths. The Navier-Stokes equations with the Spalart-Allmaras turbulence model were solved to simulate the flow structure around the Gurney flap. The computational results show that the presence of the Gurney flap can dramatically improve the tiltrotor wing lift coefficient. Compared with the baseline configuration, the maximum lift coefficient is increased by 10.67, 15.33, and 20.67% for the 1, 2, and 4% height Gurney flaps. On the other hand, the Gurney flap also results in a drag penalty, and the overall effect on the wing lift-to-drag is detrimental. In particular, at an angle of attack of 2°, use of a 4% chord length Gurney flap decreases the lift-to-drag ratio by 31.47%. Further studies demonstrate that the wing lift increments are proportional to the square root of the Gurney flap height.

1. Introduction

The modern tiltrotor aircraft is a unique type of aerial vehicle which combines the hover capability of the helicopter with the high-speed cruise performance of fixed-wing aircraft. It has wide application in military and civilian fields. Tiltrotor aircraft rely on wings and rotors for generating lift. During the conversion process, the rotors which produce the lift in the helicopter mode gradually transition to provide thrust in the airplane mode. If the wing-generated lift is not enough to overcome the aircraft gravity, the flight height can decrease, which may lead to serious crashes in some cases [1]. To furnish the required lift no longer guaranteed by the rotors, the design of wing lift-enhancement devices is a key issue for tiltrotor aircraft aerodynamics.

One of the simplest lift augmenting devices is a Gurney flap (GF) [2]. The GF is a small tab mounted at the trailing edge on the pressure side of a lifting surface. It was first studied by Liebeck [3] and was followed up by extensive wind-tunnel tests and numerical computations. Researches have elucidated impacts of their height, mounting position, orientation, and thickness. Jeffrey et al. [4] conducted experiments on the E423 airfoil with GF. Their results indicated that GF can increase the effective camber of the airfoil, thereby resulting in lift increment. The computations carried out by Singh et al. [5] showed that the GF height is a contributing factor, and the larger the GF height, the more the lift improves. The investigations were performed by Jain et al. [6] to determine the influences of chordwise locations and mounting angles on the aerodynamic characteristics of a NACA 0012 airfoil. Seven positions and seven mounting angles were systematically analyzed. It has been documented that GF should be fitted perpendicular to the chord line and as close to the trailing edge as possible to gain the maximum lift enhancement. The results of Li et al. [7] also revealed that when shifted forward from the airfoil trailing edge, the capability of GF on lift augmentation will be reduced. The effect of GF thickness has been studied by Hao and Gao using

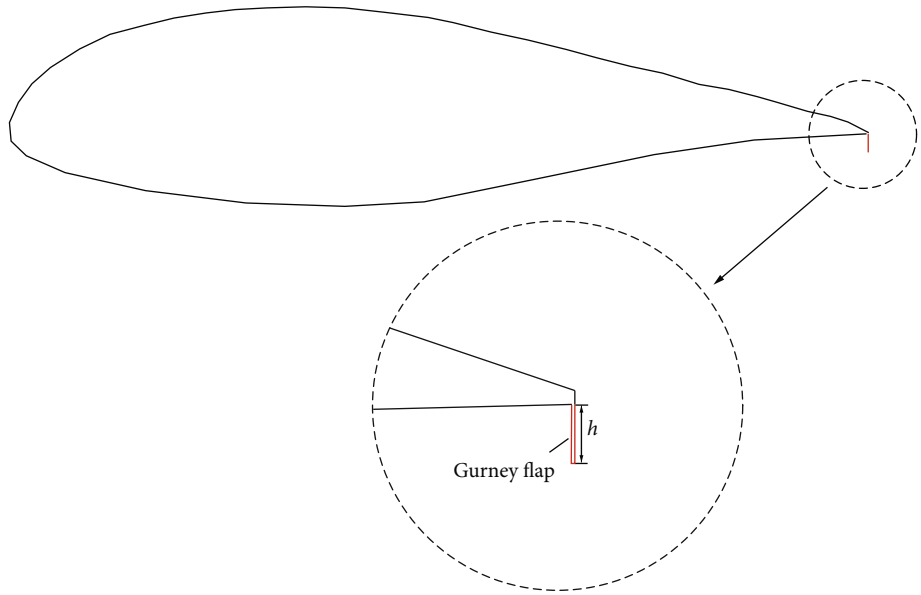

Figure 1: Gurney flap on tiltrotor wing section.

numerical simulations [8]. Based on their results, it was observed that GF thickness has a little impact on the lift coefficient and surface pressure distribution. A similar conclusion was found by Zhu et al. [9]. Although many scholars have proven that GF has a positive effect on improving lift, it increases drag simultaneously. In addition, the GF has a tendency to produce additional nose-down pitching moment [10]. To mitigate these side effects, Cole et al. [11] suggested that GF should be retracted into the airfoil when not needed. A more detailed description of the GF advantages and disadvantages can be seen in the review paper by Wang et al. [12].

Although there have been a number of studies on the effect of Gurney flaps, most of them were limited to two-dimensional airfoils or three-dimensional straight wings; few studies have been conducted on tiltrotor wings. As is well-known, lift enhancement is very necessary for tiltrotor aircraft to ensure flight safety and stability. To this end, the purpose of the current work is to investigate the lift-enhancing capability of Gurney flaps on a tiltrotor wing. Section 2 illustrates the geometry modeling and grid generation. Numerical methods are briefly described in Section 3. The quantified lift enhancement effect introduced by the GF is shown in Section 4. Conclusions are presented in the final part.

2. Geometry Modeling and Grid Generation

A realistic V-22 tiltrotor wing configuration is chosen as a basis for the numerical model. This wing is of constant cross-section with a squared tip, and the wing section is an A821201 airfoil with a thickness/chord ratio of 23%. Normalized by the wing chord length (c), the effective wing semispan is 2.75. Due primarily to structural design considerations, the wing forward sweep angle is 6° and the dihedral angle is 3.5° [13]. In the present simulation, three different GF heights (h) were studied, 1, 2, and 4% of the wing chord length. A typical GF configuration on the tiltrotor wing section is illustrated in Figure 1. All computations were performed using an O-H type grid system, as seen in Figure 2. The flow is assumed to be symmetric about the midspan. The outer boundaries are 50 chord lengths from the wing surface in the upstream, downstream, top, and bottom. The spanwise boundary is extended to 30 chord lengths away. Fine spacing ($1 \times 10^{-6}c$) in a direction normal to the wing surface is used so as to better capture the boundary layer. Figure 3 shows the surface grid of the wing and symmetry plane.

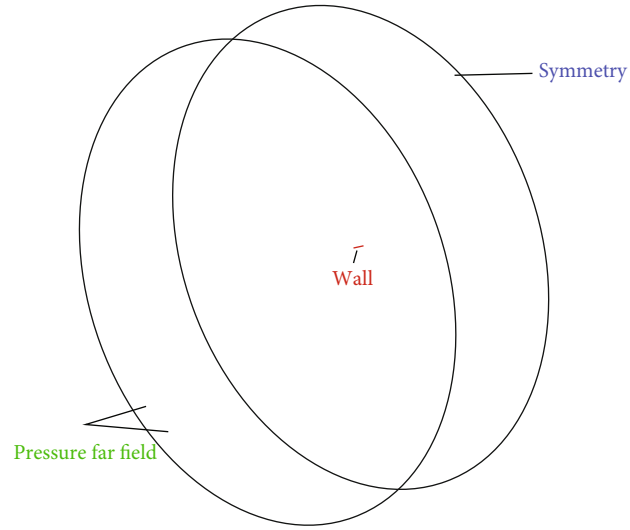

Figure 2: Mesh topology.

3. Numerical Method and Validation

3.1. Governing Equations. The flow field is governed by a Reynolds-averaged Navier-Stokes (RANS) equation, and

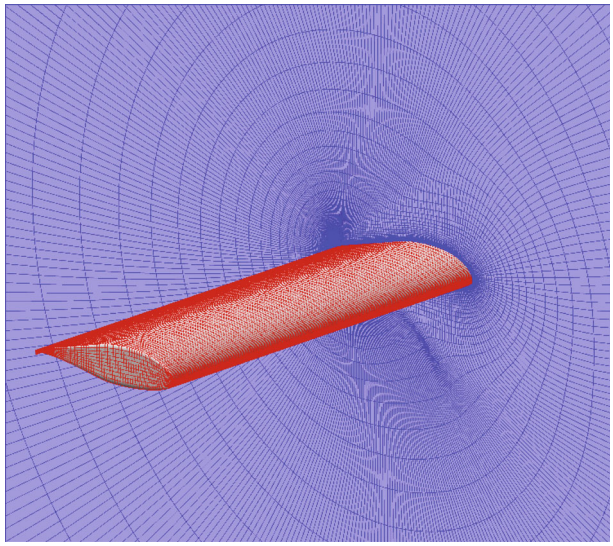

Figure 3: Wing and symmetry plane grid.

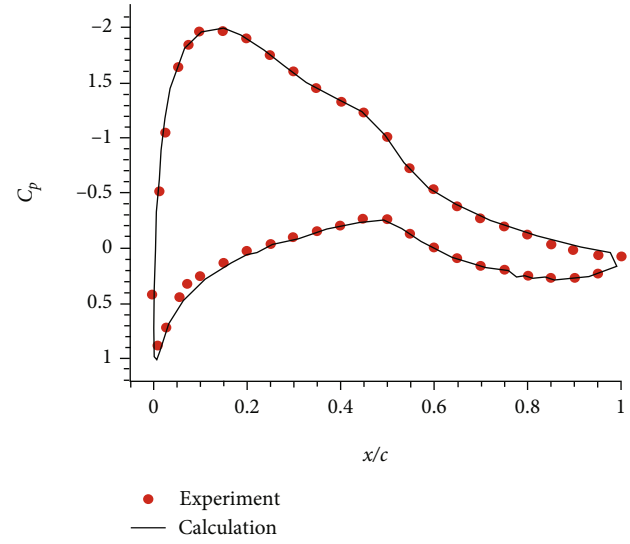

Figure 4: Comparison of pressure distributions of an A821201 infinite-straight wing.

the three-dimensional RANS equation in a conservative differential form is shown as follows [14]:

$$\frac{\partial \mathbf{W}}{\partial t} + \frac{\partial \mathbf{f}}{\partial x} + \frac{\partial \mathbf{g}}{\partial y} + \frac{\partial \mathbf{q}}{\partial z} = \frac{\partial \mathbf{R}}{\partial x} + \frac{\partial \mathbf{S}}{\partial y} + \frac{\partial \mathbf{T}}{\partial z}, \quad (1)$$

where $\mathbf{W}$ is the vector of conservative variables and expressed as

$$\mathbf{W} = \begin{bmatrix} \rho \\ \rho u \\ \rho v \\ \rho w \\ \rho E \end{bmatrix}. \quad (2)$$

$\mathbf{f}$, $\mathbf{g}$, and $\mathbf{q}$ are the convective flux vectors formulated as

$$\mathbf{f} = \begin{bmatrix} \rho u \\ \rho u^2 + p \\ \rho uv \\ \rho uw \\ \rho uE + up \end{bmatrix}, \quad \mathbf{g} = \begin{bmatrix} \rho v \\ \rho vu \\ \rho v^2 + p \\ \rho vw \\ \rho vE + vp \end{bmatrix}, \quad \mathbf{q} = \begin{bmatrix} \rho w \\ \rho wu \\ \rho wv \\ \rho w^2 + p \\ \rho wE + wp \end{bmatrix}. \quad (3)$$

Here, p is the pressure, ρ is the density, and E is the total energy per unit mass; u, v, and w are the Cartesian velocity components; $\mathbf{R}$, $\mathbf{S}$, and $\mathbf{T}$ are the viscous flux vectors. The finite volume method was applied for the spatial discretization with a second-order accuracy central difference scheme, and the dual time-stepping strategy was implemented to the unsteady flow simulations. The Spalart-Allmaras model [15] was selected as the turbulence model for all results discussed here. As for boundary conditions, the surface boundaries of the wing and GF are defined as the no-slip wall condition, and symmetry is enforced at the midspan. At the far-field surface, the characteristic-based nonreflecting boundary condition was applied.

3.2. Validation

3.2.1. Infinite-Straight Wing. The first validation case is an infinite straight wing. The airfoil profile is exactly that employed in the V-22 tiltrotor aircraft. In this case, the chord Reynolds number is 2.0×10^6 (Mach number 0.13), and the angle of attack is 7°. Comparison between the numerical chordwise pressure distribution and the measured data [16] is shown in Figure 4. Very good agreement between the computed results and the experimental values is observed.

3.2.2. NACA 0012 Wing with Gurney Flap. Due to the lack of experimental data of the tiltrotor wing with Gurney flaps, present numerical modelling is validated against the experimental data of a NACA 0012 wing. The model has an aspect ratio of 1.6, and the flow conditions for simulation are the same as those of the wind-tunnel test [17]. Comparison of computed aerodynamic coefficients with experimental data is depicted in Figure 5, and Figure 6 shows a good agreement between the computed and measured pressure distributions without and with a 2%c height GF. These results demonstrate that the present numerical approach is satisfactory to obtain the accurate aerodynamic characteristics of the wing with GFs.

4. Results and Discussion

In this work, three different GF heights were studied on the semispan V-22 tiltrotor wing. They are 1, 2, and 4% of the wing chord length. All calculations were conducted at a Mach number of 0.2, yielding a Reynolds number of 4.65×10^6 based on the reference chord length.

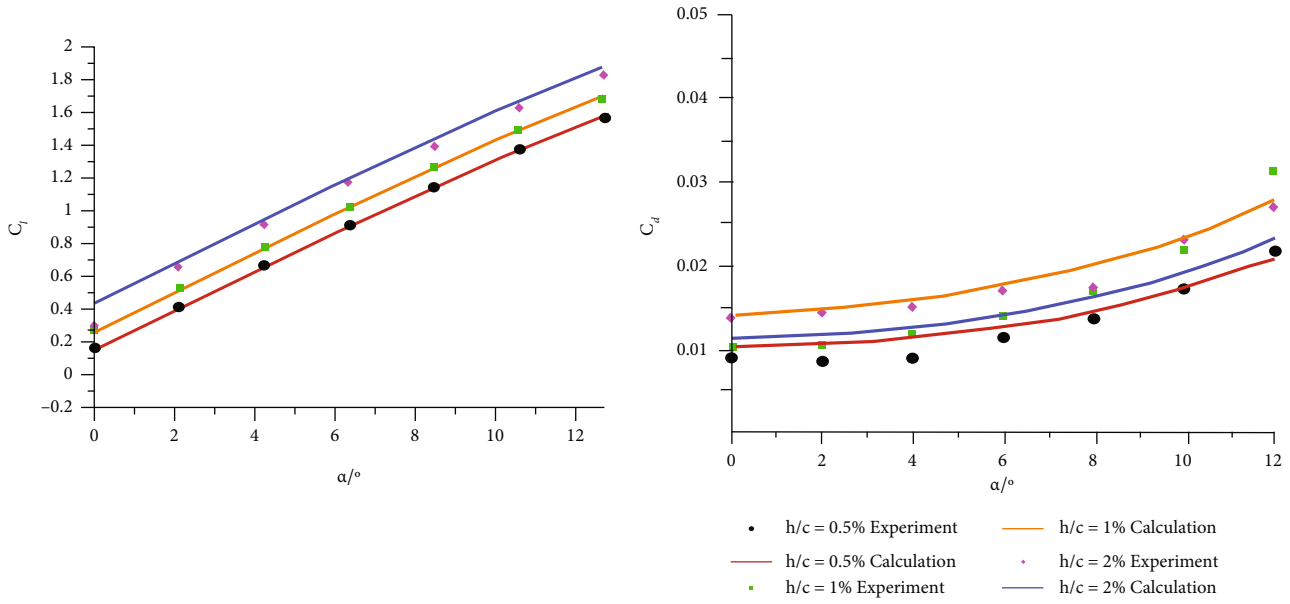

(a) Lift curves (b) Drag curves

Figure 5: Aerodynamic coefficients of a NACA 0012 wing with different GFs.

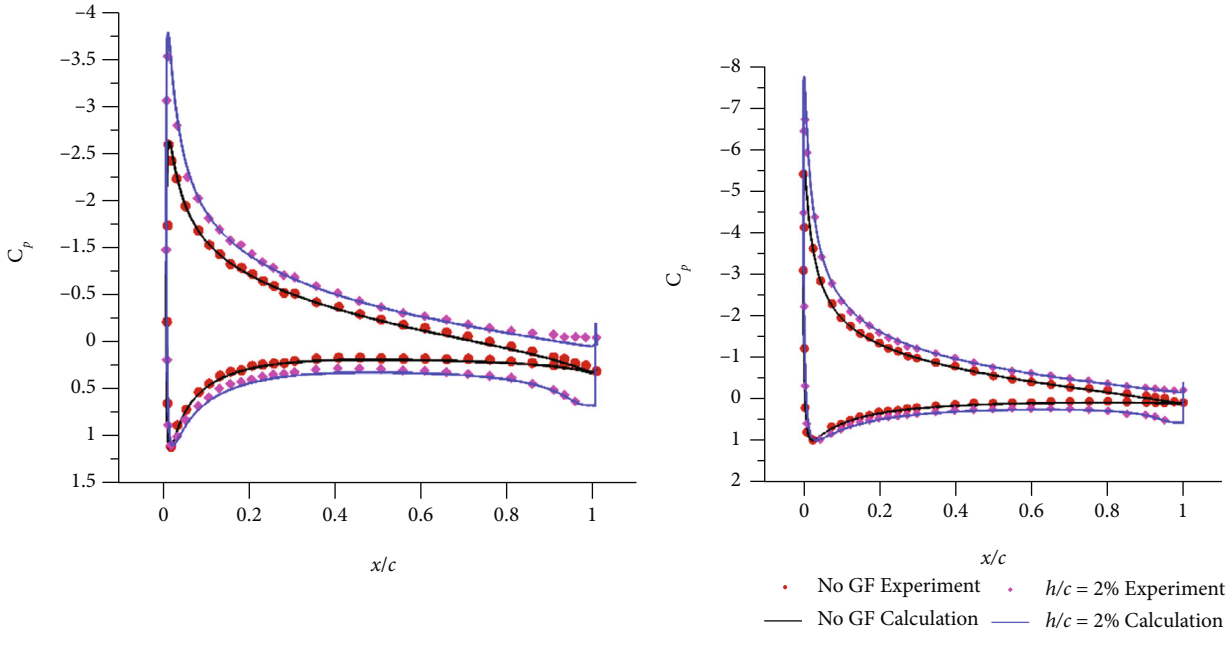

(a) $\alpha = 6°$ (b) $\alpha = 10°$

Figure 6: Calculated and experimental pressure distributions of a NACA 0012 wing without and with GF.

Table 1: Mesh dependency study of tiltrotor wing with a 2%c GF at $\alpha = 8°$.

	Total number of grid	C_l	C_d	C_m
Coarse	1,860,000	1.23670	0.11165	0.00924
Medium	3,670,000	1.23998	0.11156	0.00951
Fine	7,150,000	1.23972	0.11149	0.00952

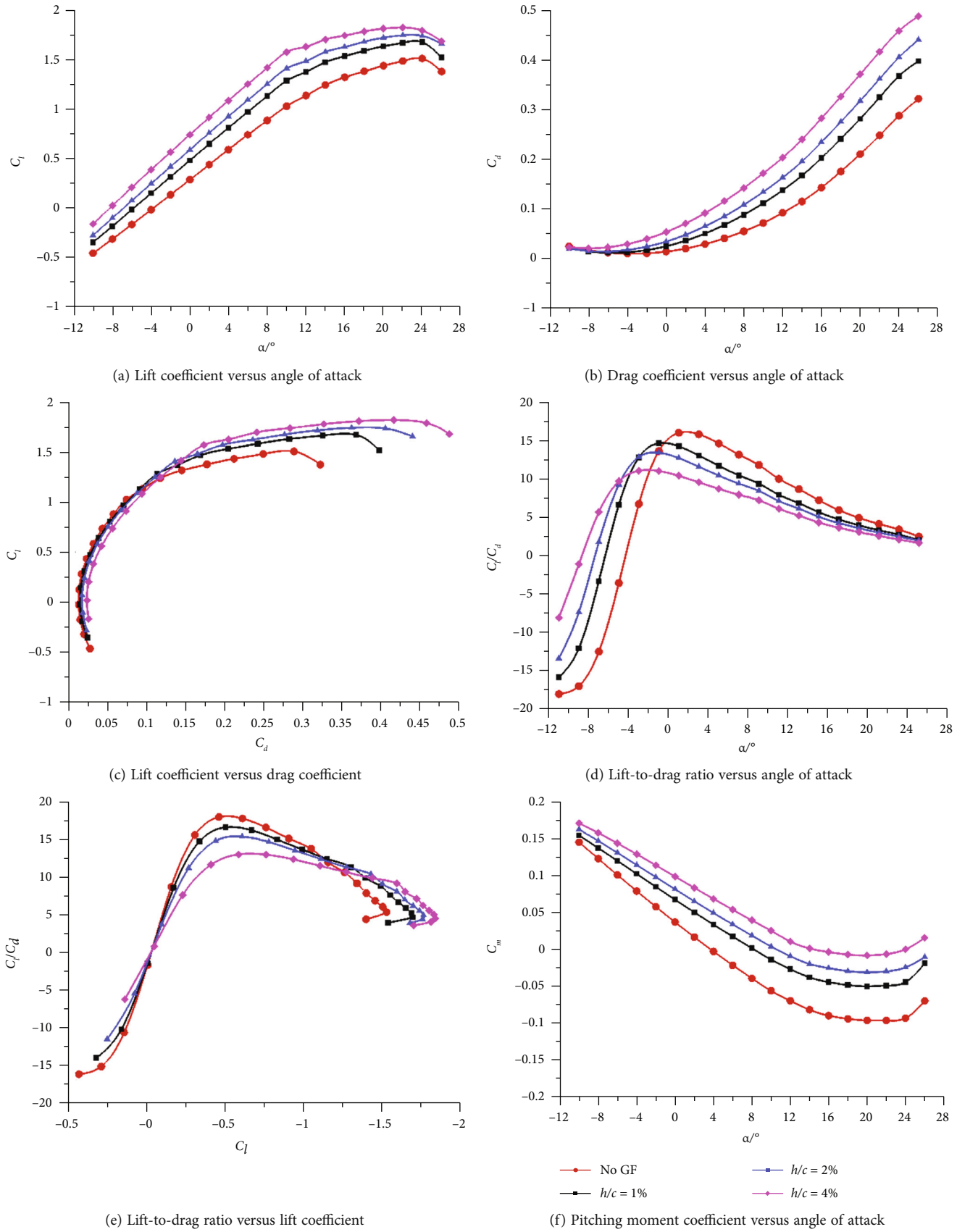

(a) Lift coefficient versus angle of attack

(b) Drag coefficient versus angle of attack

(c) Lift coefficient versus drag coefficient

(d) Lift-to-drag ratio versus angle of attack

(e) Lift-to-drag ratio versus lift coefficient

(f) Pitching moment coefficient versus angle of attack

Figure 7: Effect of GF height on wing aerodynamic coefficients.

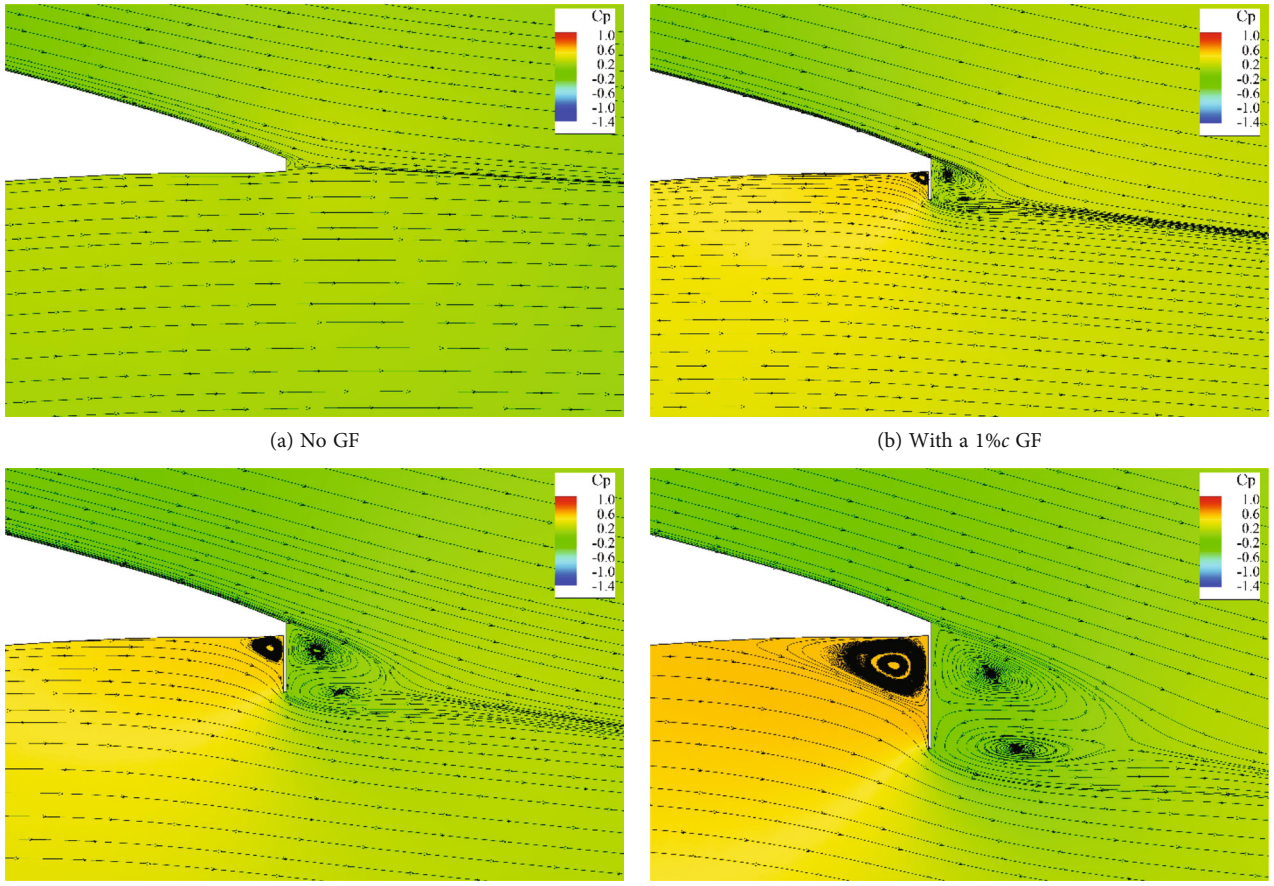

(a) No GF (b) With a 1%c GF

(c) With a 2%c GF (d) With a 4%c GF

FIGURE 8: Pressure contours and flow structure near the trailing edge in the wing root plane at $\alpha = 0^{\circ}$.

4.1. Mesh Dependency Study. To check the accuracy of the mesh resolution, mesh dependency studies are carried out. Three types of grids are compared: 1,860,000 (coarse), 3,670,000 (medium), and 7,150,000 (fine). The computed aerodynamic coefficients are given in Table 1. It is shown that the differences between the medium grid and the fine grid are negligible. Therefore, the medium grid is used for the present simulation.

4.2. Effects of Gurney Flap on Aerodynamic Characteristics. The lift coefficients (C_l) versus the angle of attack (α) without and with a GF are shown in Figure 7(a). Obviously, lift augmentation is observed with the implementation of GF. The increment of C_l is more remarkable with larger GF height. Compared to the baseline wing, the maximum lift coefficient ($C_{l,\max}$) is increased by 10.67, 15.33, and 20.67 for the 1, 2, and 4% height Gurney flaps, respectively. For the $h/c = 2$ and 4% cases, the stall angle (α_{stall}) is decreased from 24° to 22°. When a larger GF is utilized, the zero-lift angle of attack (α_{ZL}) appears to become increasingly more negative. Moreover, the lift-curve slope ($C_{l\alpha}$) for the controlled configurations is found to be higher than that of the clean wing. These results thus show that GF serves to add the effective camber of the wing.

Figure 7(b) presents the drag coefficient (C_d) as a function of the angle of attack, and the drag polar curve is shown in Figure 7(c). It is quite clear that GF increases the drag coefficient for all angles of attack, and the larger the GF height is, the more the drag increase will be. Substantial drag

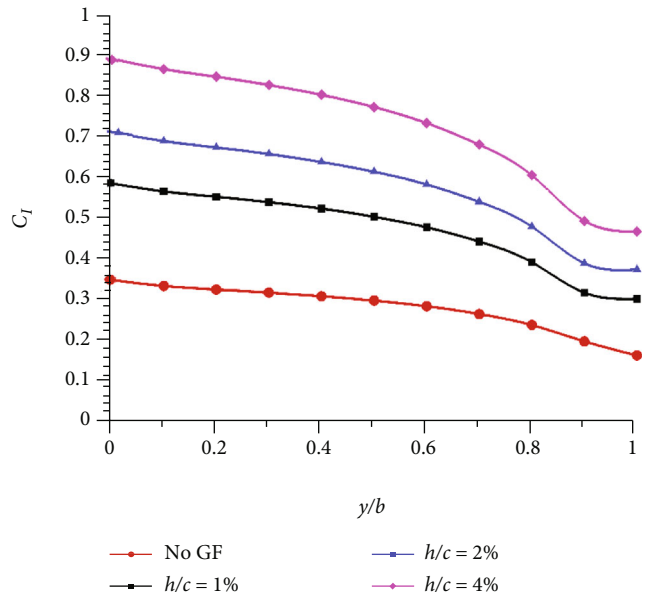

FIGURE 9: Effect of GF height on sectional lift coefficient at $\alpha = 0^{\circ}$.

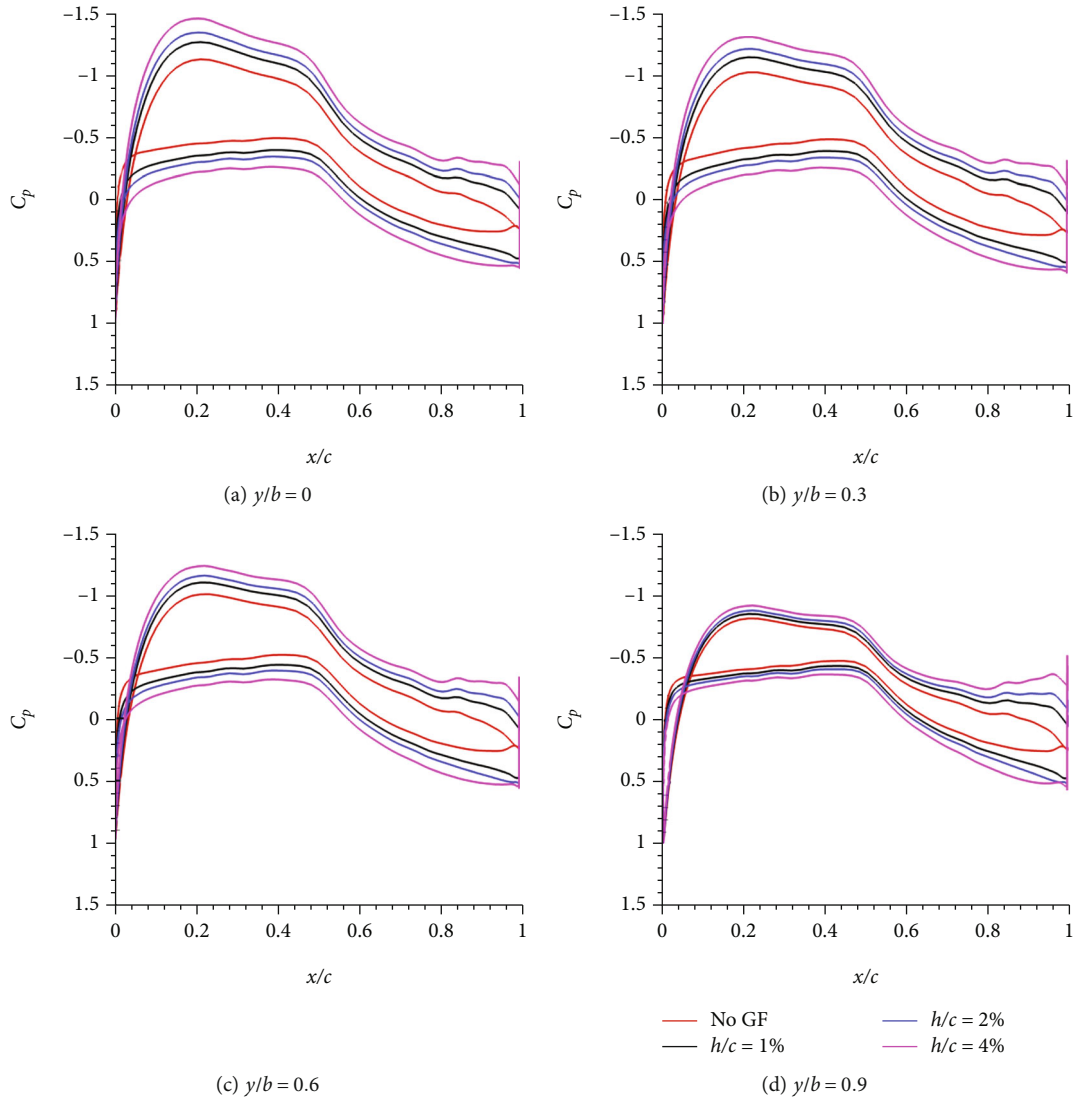

Figure 10: Pressure coefficient distributions on different spanwise locations at $\alpha = 0^\circ$.

Table 2: Aerodynamic performance parameters of tiltrotor wing without and with a GF.

Configuration	$C_{l\alpha}$	$C_{l,\max}$	α_{stall}	$(C_l/C_d)_{\max}$	α_{ZL}	$C_{d,\min}$
No GF	4.28 rad^{-1}	1.50	24°	17.72	-3.66°	1.41×10^{-2}
$h/c = 1\%$	4.69 rad^{-1}	1.66	24°	16.36	-5.71°	1.59×10^{-2}
$h/c = 2\%$	4.83 rad^{-1}	1.73	22°	15.14	-6.76°	1.84×10^{-2}
$h/c = 4\%$	4.97 rad^{-1}	1.81	22°	12.79	-8.17°	2.46×10^{-2}

increment is observed when the height is increased to 4%c. This is in agreement with the results of Singh et al. [5]. To some extent, because the required time for the transition from helicopter mode to airplane mode is short, the drag penalty caused by the GF is acceptable.

Figures 7(d) and 7(e) show the characteristics of the lift-to-drag ratio (C_l/C_d) at different GF heights. Because GF produces more drag than the clean one, the lift-to-drag ratio of the controlled wing is greatly reduced. In comparison with the baseline wing at $\alpha = 2^\circ$, which is about the cruising angle for the tiltrotor aircraft, the lift-to-drag ratio is decreased by 9.88, 18.49, and 31.47% with 1, 2, and 4% height Gurney flaps, respectively. According to the voyage equation [18], the lift-to-drag ratio in the forward-flight mode plays an important role in the flight range. As a result, in order to use the GF efficiently, it is recommended that the GF should be closed at cruise. Figure 7(f) shows the effect of the Gurney flap's height on the pitching moment.

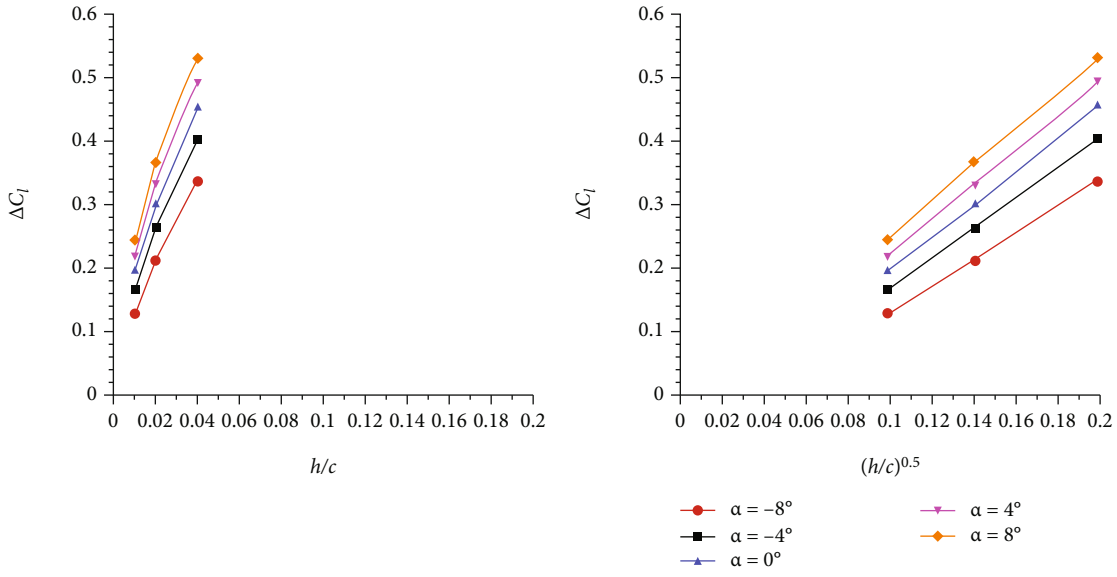

(a) Lift coefficient increments versus h/c

(b) Lift coefficient increments versus $(h/c)^{0.5}$

Figure 11: Variation of lift coefficient increment with GF relative height.

To better understand the flow mechanism of the GF, Figure 8 presents the pressure contours and streamlines in the vicinity the trailing edge at $\alpha = 0°$. Without a GF, as shown in Figure 8(a), the streamlines are in general very smooth. When a GF is installed, as shown in Figures 8(b)–8(d), three vortices, one upstream of the GF and two counter-rotating vortices downstream of the GF, can be clearly seen. The Kutta condition shifts from the airfoil trailing edge to the lower edge of the GF, which leads to lift enhancement [19]. Moreover, because the windward side of the GF endures high pressure and the leeward side endures low pressure, the drag increases with the existence of a GF. The spanwise lift distribution is shown in Figure 9. Four different spanwise locations are selected for further analyzing the chordwise pressure variation. These locations are placed at $y/b = 0$, 0.3, 0.6 and 0.9 from the wing root, where b is the wing span length. Figure 10 presents the pressure distributions for various positions without and with a GF. It is evident that the addition of GF increases the pressure difference between the upper and lower surfaces of the wing section, especially near the wing root.

To deeply determine the effect of the GF, Table 2 lists the lift-curve slope, the maximum lift coefficient, the stall angle, the maximum lift-to-drag ratio, the zero-lift angle of attack, and the minimum drag coefficient ($C_{d,\min}$) for the uncontrolled and controlled tiltrotor wing. On the whole, GF improves the lift-curve slope and maximum lift coefficient and decreases the stall angle and maximum lift-to-drag ratio. Additionally, as the height of the GF increases, the zero-lift angle of attack becomes more negative, and the minimum drag coefficient increases. Data points from -8° to 8° are employed to evaluate the relationship between the lift coefficient increment (ΔC_l) and GF height (h/c). The variation of ΔC_l versus h/c as well as $(h/c)^{0.5}$ is displayed in Figure 11. The results show that the lift increments are nonlinear with respect to GF height (see Figure 11(a)). In contrast, it is very interesting to find that the lift improvements are proportional to the square root function of the GF height, as shown in Figure 11(b), which is similar with the results in Ref. [20].

5. Conclusions

The aerodynamic characteristics of the tiltrotor wing without and with a GF were comprehensively investigated using numerical simulations. Different GF sizes between 1 and 4% of the wing chord have been studied. The aerodynamic performance parameters were analyzed qualitatively and quantitatively. As expected, the results show that GF is an efficient lift augmentation device, and the larger the GF height is, the more obvious the lift-enhancement will be. The drag coefficient is also increased with the introduction of a GF, and the overall effect on the wing lift-to-drag ratio is detrimental. Further analysis indicates that the lift improvement associated with a GF is related to the square root of the GF height. Conclusions acquired in this study may provide some guidance for the design of tiltrotor aircraft aerodynamics.

Data Availability

The data used to support the findings of this study are available from the corresponding author upon request.

Conflicts of Interest

The authors declare that there is no conflict of interest regarding the publication of this paper.

Acknowledgments

This work was supported by the Natural Science Foundation of the Jiangsu Higher Education Institutions of China (No. 21KJB130003) and the Scientific Research Foundation of Huaiyin Institute of Technology (No. Z301B19511).

References

[1] Z. Liu, Y. He, L. Yang, and J. Han, "Control techniques of tilt rotor unmanned aerial vehicle systems: a review," *Chinese Journal of Aeronautics*, vol. 30, no. 1, pp. 135–148, 2017.

[2] L. Daniel and L. W. Traub, "Effect of aspect ratio on Gurney-flap performance," *Journal of Aircraft*, vol. 50, no. 4, pp. 1217–1225, 2013.

[3] R. H. Liebeck, "Design of subsonic airfoils for high lift," *Journal of Aircraft*, vol. 15, no. 9, pp. 547–561, 1978.

[4] D. Jeffrey, X. Zhang, and D. W. Hurst, "Aerodynamics of Gurney flaps on a single-element high-lift wing," *Journal of Aircraft*, vol. 37, no. 2, pp. 295–301, 2000.

[5] M. K. Singh, K. Dhanalakshmi, and S. K. Chakrabartty, "Navier-Stokes analysis of airfoils with Gurney flap," *Journal of Aircraft*, vol. 44, no. 5, pp. 1487–1493, 2007.

[6] S. Jain, N. Sitaram, and S. Krishnaswamy, "Computational investigations on the effects of Gurney flap on airfoil aerodynamics," *International Scholarly Research Notices*, vol. 2015, Article ID 402358, 11 pages, 2015.

[7] Y. Li, J. Wang, and P. Zhang, "Influences of mounting angles and locations on the effects of Gurney flaps," *Journal of Aircraft*, vol. 40, no. 3, pp. 494–498, 2003.

[8] L. S. Hao and Y. W. Gao, "Effect of Gurney flap geometry on a S809 airfoil," *International Journal of Aerospace Engineering*, vol. 2019, Article ID 9875968, 8 pages, 2019.

[9] H. Zhu, W. Hao, C. Li, S. Luo, Q. Liu, and C. Gao, "Effect of geometric parameters of Gurney flap on performance enhancement of straight-bladed vertical axis wind turbine," *Renewable Energy*, vol. 165, pp. 464–480, 2021.

[10] T. Lee and Y. Y. Su, "Lift enhancement and flow structure of airfoil with joint trailing-edge flap and Gurney flap," *Experiments in Fluids*, vol. 50, no. 6, pp. 1671–1684, 2011.

[11] J. A. Cole, B. A. O. Vieira, J. G. Coder, A. Premi, and M. D. Maughmer, "Experimental investigation into the effect of Gurney flaps on various airfoils," *Journal of Aircraft*, vol. 50, no. 4, pp. 1287–1294, 2013.

[12] J. J. Wang, Y. C. Li, and K. S. Choi, "Gurney flap–lift enhancement, mechanisms and applications," *Progress in Aerospace Sciences*, vol. 44, no. 1, pp. 22–47, 2008.

[13] H. Rosenstein and R. Clark, "Aerodynamic development of the V-22 tilt rotor," in *Aircraft Systems*, p. 2678, Design and Technology Meeting, Dayton, Ohio, 1986.

[14] H. Chen, "Numerical calculations on the unsteady aerodynamic force of the tilt-rotor aircraft in conversion mode," *International Journal of Aerospace Engineering*, vol. 2019, Article ID 2147068, 15 pages, 2019.

[15] P. Spalart and S. Allmaras, "A one-equation turbulence model for aerodynamic flows," in *30th Aerospace Sciences Meeting and Exhibit*, Reno, Nevada, 1992.

[16] M. D. Jenks and J. C. Narramore, *Final report for the 2-D test of model 901 rotor and wing airfoils (BSWT 592)*, Bell-Boeing Tiltrotor Team, Rept. D901-99065-1, 1984.

[17] Y. C. Li, J. J. Wang, and P. Zhang, "Effects of Gurney flaps on a NACA0012 airfoil flow," *Turbulence and Combustion*, vol. 68, no. 1, pp. 27–39, 2002.

[18] T. Zhang, Z. Wang, W. Huang, and L. Yan, "Parameterization and optimization of hypersonic-gliding vehicle configurations during conceptual design," *Aerospace Science and Technology*, vol. 58, pp. 225–234, 2016.

[19] X. He, J. J. Wang, M. Q. Yang, D. L. Ma, C. Yan, and P. Q. Liu, "Numerical simulation of Gurney flaps lift-enhancement on a low Reynolds number airfoil," *SCIENCE CHINA Technological Sciences*, vol. 60, no. 10, pp. 1548–1559, 2017.

[20] T. Liu and J. Montefort, "Thin-airfoil theoretical interpretation for Gurney flap lift enhancement," *Journal of Aircraft*, vol. 44, no. 2, pp. 667–671, 2007.